International Journal on Advanced Science Engineering Information Technology

Vol.12 (2022) No. 5
ISSN: 2088-5334

Horizontal and Vertical Geometric Accuracy of Agisoft Photoscan and Pix4D Mapper Softwares at Kebun Raya Universitas Mulawarman in Samarinda, East Kalimantan, Indonesia

Sri Endayani [a,*], Ronggo Sadono [b], Ambar Kusumandari [b], Hartono [c], M. Baiquni [c]

[a] *Faculty of Agriculture, Universitas 17 Agustus 1945, Samarinda. 75123, Indonesia*
[b] *Faculty of Forestry, Universitas Gadjah Mada, Yogyakarta 55281, Indonesia*
[c] *Faculty of Geography, Universitas Gadjah Mada, Yogyakarta 55281, Indonesia*
*Corresponding author: *enda@untag-smd.ac.id*

***Abstract*— The advent of unmanned aerial vehicles has improved aerial photography, which is now aided by computer software for data acquisition and processing. These developments allow for accurate aerial photographs of Kebun Raya Universitas Mulamarwan Samarinda (KRUS) for managerial purposes. This study aims to compare the accuracy of horizontal and vertical geometry with Agisoft Photoscan (AP) and Pix4D Mapper (PM) software. The materials consisted of 150 aerial photographs of KRUS with eight ground control points (GCP) and one internal control point (ICP). Data were obtained from nine flight paths with AP and PM software linked to GCP and ICP. These data were processed and compared to manual measurements using linear error (LE) 90 and circular error (CE) 90 criteria. The commission omission equation was used for the object accuracy test on orthophoto. The vertical geometry accuracy test was carried out using the criteria of root mean square error (RMSE) and LE90 values on the digital elevation model. In comparison, the horizontal geometry accuracy test was performed by using the obtained orthophoto based on RMSE and CE90 criteria. The result demonstrated that the horizontal geometry accuracy for AP was higher than PM, indicated by lower RMSE and CE90 values, which were 0.091 versus 0.148 and 0.139 versus 0.224 for AP and PM, respectively. The vertical geometry accuracy was similar, with lower RMSE and LE90 values of 0.169 versus 0.309 and LE90 0.279 versus 0.224 for AP and PM, respectively. Furthermore, AP is a potential tool for KRUS spatial mapping.**

***Keywords*—Ground and internal control point; digital elevation model; orthophoto; linear and circular error; commission omission equation.**

Manuscript received 28 Sep. 2021; revised 15 Dec. 2021; accepted 15 Feb. 2022. Date of publication 31 Oct. 2022.

I. INTRODUCTION

Aerial photography technology continues to develop rapidly, effectively, and efficiently. The development of aerial photography is aided by computer software for data retrieval and processing [1]–[3]. The most recent photogrammetric technology for mapping purposes today is the use of unmanned aerial vehicles (UAV) for mapping areas [4]–[6]. Compared to earlier mapping technologies, this technology has various advantages, including a shorter processing time, a simpler and easier-to-transport design, and a high level of accuracy [7]-[9]. A UAV aircraft is a light and small aircraft controlled by a remote-control system using radio waves. In addition, it can be controlled manually or automatically using data from sensors and has the advantages of faster time, simplicity, ease of carrying, and high accuracy [10]–[12]. This photogrammetric measurement can be applied both on a small and large scale with camera systems, thermal or infrared, light detection and ranging (LiDAR), and a combination of those three above [13]–[15]. Therefore, this technological advancement is suitable for survey and mapping purposes.

Survey and mapping activities on a large scale require high accuracy in a short time. Photogrammetry can be an alternative solution. Photogrammetry serves to obtain reliable information about physical objects and the environment through recording, measuring, and interpreting photographic images from recorded electromagnetic energy radiation [9], [10]–[12], [16], [17]. Alternatively, processing aerial photographs to obtain precise data and information for mapping and engineering purposes [3]–[5]. The development of accurate and efficient photogrammetry is very beneficial in

the field of mapping [18]–[20]. In addition, mapping cannot be separated from the reference to terrestrial measurements, from setting ground controls to measuring land borders measured in the field. [23], [26], [27]. Furthermore, photogrammetry mapping enables high accuracy in topographic and parcel mapping [21]–[23]. Notably, mapping results in the form of photo maps cannot be directly used as a basis or attachment to map publications [22], [23], [26]. As a consequence, mapping techniques through aerial photography are used, namely recordings of part of the earth's surface made using cameras mounted on vehicles, including airplanes [6]–[8], [21], [24], [25]. Furthermore, aerial photographs must be processed with software such as Agisoft Photoscan (AP) and Pix4D Mapper (PM).

AP is a computer technology software in image processing algorithms and digital photogrammetric techniques that can identify mosaic coordinate points and create a digital surface model (DSM) automatically [21]–[24]. Meanwhile, Pix4D Mapper develops advanced digital photo processing algorithms and converts digital photos into ortho mosaic 2D georeferenced 3D surface and point cloud models, automatic aerial triangulation, and professional UAV data processing software [19]–[22]. The initial application of both software for photogrammetry was for photogrammetric topographic mapping [28]–[30]. Furthermore, the engineering sector utilizes photogrammetry to create maps of land tax, land, forest, geology, and urban and regional planning and zoning [31]–[33]. In addition, the fields of astronomy, architecture, ecology, mineralogy, and military information collections are the oldest users to date [34]–[36].

Kebun Raya Universitas Mulawarman Samarinda (KRUS), with a land size of 300 hectares, is geographically located at 0°25'24″ S and 117°14'14″ E. The Faculty of Forestry, Universitas Mulawarman, has authorized the use of this KRUS for instructional purposes. It is a need for managerial considerations that this KRUS be accurately mapped. Therefore, this research aims to compare the horizontal and vertical geometric accuracy of KRUS's map using AP and PM.

II. Materials and Method

A. Materials

One hundred fifty aerial photos of KRUS were used and obtained using DJI Phantom 4 Pro. This UAV-Drone was equipped with an AP that automatically regulated nine determined flight paths and an internal control point (ICP), and autopilot flight [4]–[6]. On the ground, eight stakes as static ground control points (GCP) were installed that have been connected to national reference and ICP on the Drone (Fig. 1). In addition, the length of the wide of several objects was measured with a rolling meter for further accuracy testing [23], [26], [27]. These selected objects were dormitory, house, trench wall, gutter, decker, fishpond, field, office, and road (Fig. 2). The activity of this aerial photography acquisition was completed in March of 2020.

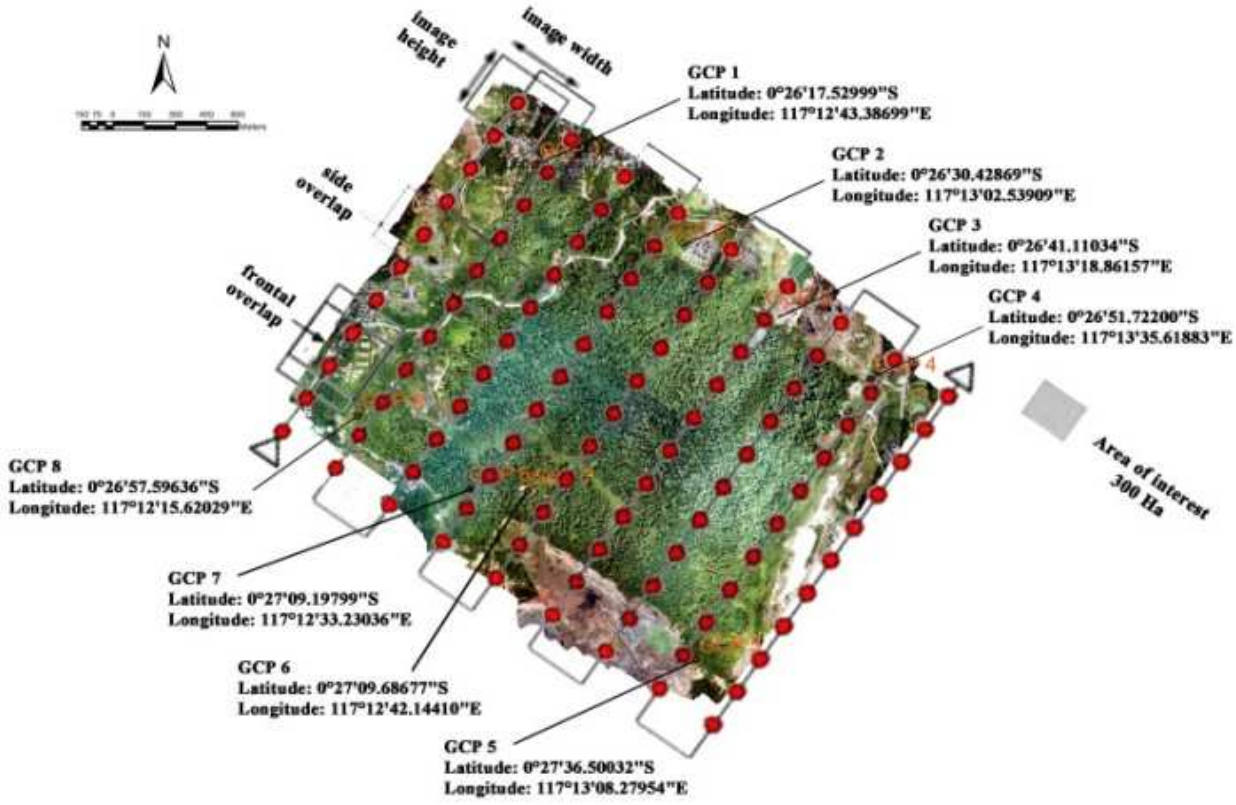

Fig. 1 Nine flight paths of DJI Phantom 4 Pro-Drone starting form Southwest (denoted with triangle) and 150 shoot points (red dot) to obtain 150 aerial photographs over Kebun Raya Universitas Samarinda with eight ground control points (GCP).

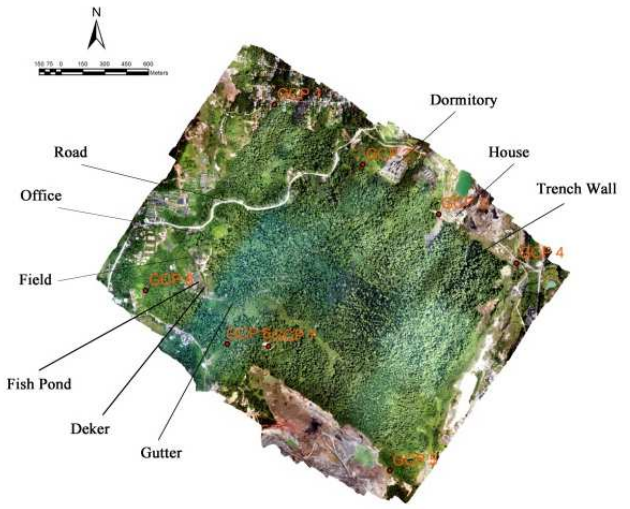

Fig. 2 The measured objects and their location for accuracy testing in clockwise order: dormitory, house, trench wall, gutter, decker, fishpond, field, office, and road

B. Methods

The 150 aerial photographs were merged to obtain one sheet of 2D photography and a georeferenced digital elevation model (DEM) of KRUS using AP and PM software, respectively (Fig. 3). In addition, both software was also used for the aerial photo orthorectification process [21]–[23]. Furthermore, the two software were used to determine the difference in geometric accuracy of the resulting orthophoto and DEM [10]–[12]. To test the accuracy of orthophoto objects, interpretations were employed, and commission equations for horizontal and vertical geometry were used [6]–[8], [21], [24], [25].

In the AP segment, the aerial acquisition photos from the AP software were merged and reconstructed based on the sequential flight path. Two or more photos were aligned to create the matching points and obtain the initial 3D visualization. The GCPs were identified, and their coordinates were imported as a reference for X, Y, and Z coordinates, which could improve the quality of DEM and orthophoto in geodetic geometry. The Build Mesh module was obtained as follows: DEM, digital surface model (DSM), digital terrain model (DTM), and Orthophoto, which were then used to create the final 3D model. Furthermore, the Build Orth mosaic module corrected geometric errors in DEM and GCP aerial photographs. Then, both DSM and DTM processes were used in the Build DEM module to convert the final 3D model to a raster or grid format.

Initial processing was the first module with the use of PM. The coordinates of GCP's were imported and then extracted to serve as key points and a reference for X, Y, and Z coordinates. Therefore, the obtained DEM and Orthophoto could be improved the geometric quality.

Further processing using Arc GIS 10.1 software was carried out in three stages simultaneously to verify the correctness of the orthophoto model. The first stage was initial processing to improve the accuracy of obtained DSM and Orth mosaic. The second stage was to increase the density of the 3D points in the 3D model. The final stage was DSM, Orth mosaic, and Indexing to convert the processed data into DSM and Orth mosaic [37], [38]. In addition, both AP and PM software were used to check the correctness of the orthophoto model, horizontal and vertical geometry [15], [39], [40]. Furthermore, the next process was to proceed with the accuracy of orthophoto objects.

The accuracy of geometry describes the difference between the coordinates of an object's position on a map and its actual position. The criterion for this accuracy includes a circular error (CE) and linear error (LE) with a 90% confidence level for horizontal or orthophoto accuracy and vertical or DEM accuracy, respectively. The accuracy of CE90 and LE90 values described that the horizontal and vertical error did not exceed 90% confidence level. In addition, two-dimensional mapping considers the field's X and Y coordinates, key points, and positions. Furthermore, the root means square error (RMSE) was used for positional accuracy, which describes the value of the difference between the test point and the GCP point and the random accuracy of objects [17].

The accuracy test refers to the difference in X, Y, and Z coordinates between the aerial photo test points and objects in the field using RMSE for CE and LE. The accuracy of aerial images was tested by placing key point items in the field and matching these photographed objects on the processed aerial photographs using the following Formula 1a & 1b [17].

The square root of the average square of the difference between the coordinate data values and the coordinate values from an independent source with better precision is the root mean square error (RMSE).

1) RMSE Calculation:

$$RMSE_{horisontal} = \sqrt{\frac{D^2}{n}}$$

$$D^2 = \sqrt{RMSE_X^2}\, RMSE_Y^2 = \sqrt{\frac{D\,(X_{data}X_{cek})^2 (Y_{data}Y_{cek})^2}{n}}$$

$$RMSE_{horisontal} = \sqrt{\frac{D(Z_{data}Z_{cek})^2}{n}} \qquad (1a)$$

Where:

n = Total number of checks on the map
D = The difference between the coordinates measured in the field and the coordinates on the map
x = Coordinate value on X. axis
y = Coordinate value on Y. axis
z = Coordinate value on the Z-axis

The circle's radius indicates that 90 percent of the error or difference in the horizontal position of objects on the map with the assumed actual position is not greater than that radius. Circular Error 90 percent (CE90) is a measure of horizontal geometric accuracy that is defined as the radius of a circle indicating that 90 percent of the error or difference in the horizontal position of objects on the map with the assumed actual position is not greater than that radius. Linear Error 90 percent (LE90) is a distance number indicating that 90 percent of the error or discrepancy in the height value of objects on the map with the real height value is not more than the distance value. The formula for calculating CE90 and LE90 values is:

$$CE90 = 1{,}5175\; x\; RMSE_r$$
$$LE90 = 1{,}6499\; x\; RMSE_z \qquad (1b)$$

2) Orthophoto model accuracy test: Aerial photography scale refers to the distance of aerial photographs on the ground, camera focal length, and altitude of flight to objects from sea level in the process of forming DSM, Orth mosaic, and index using formula 2 [10]–[12].

$$S = \frac{ab}{AB} = \frac{f}{H'} = \frac{f}{H-h} \quad (2)$$

Where:

S = Aerial photography scale
ab = Distance in aerial photography
AB = Distance in the field/field
f = Camera focal length
H' = Airplane's flying height concerning object/field
H = Altitude of the vehicle flying
h = The height of the object above sea level (asl)

3) Geometric accuracy analysis: Aerial photography produces a central projection of varying scales from the heights of different locations and then averages (average photo scale). Comparing the camera focal length and flight altitude to the average location height, formula 3 [15], [39], [40].

$$S\ average = \frac{f}{H-h\ average} \quad (3)$$

Where:

f = Camera focal length
H = The altitude of the vehicle flying
h = Height of object/field from sea level (asl)
S = Scale

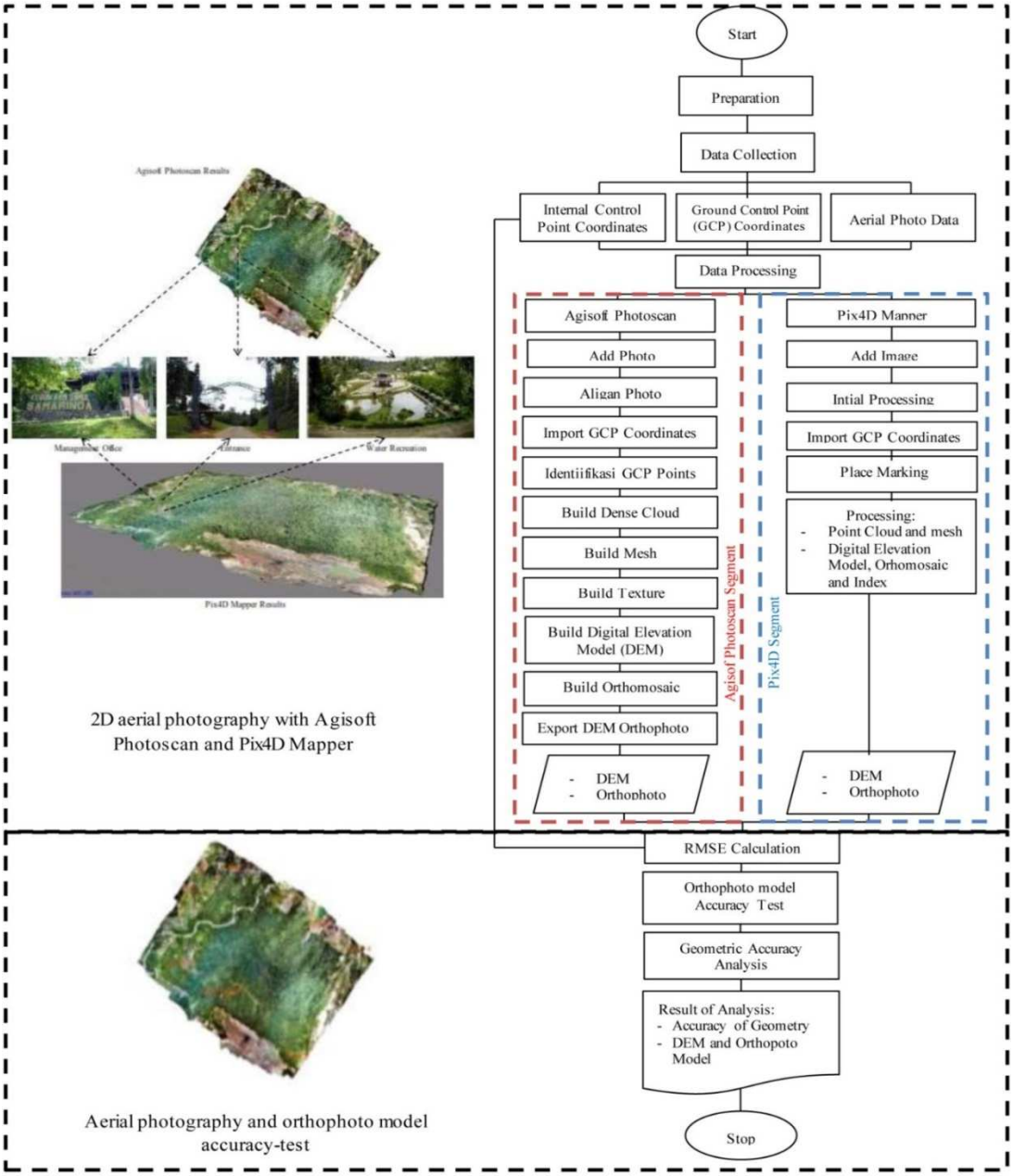

Fig. 3 Sequential workflow to compare horizontal and vertical geometry accuracy between Agisoft Photoscan and Pix4D Maper softwares at Kebun Raya Universitas Mulawarman, Samarinda

III. Results and Discussion

A. Aerial Photography with AP and PM

Orthophoto and DEM data were the results of aerial photo processing. The orthophotos generated by the AP (Fig. 4) and PM (Fig. 5) software looked exactly like the actual item shapes in the investigated field.

Fig. 4 Visualization of orthophoto by the use of Agisoft Photoscan

Fig. 5 Visualization of orthophoto by the use of Pix4D Mapper

Furthermore, a similar result also occurred on both 2D and 3D DEM obtained using AP (Fig. 6) and PM (Fig. 7), showing no difference in elevation or image shape from aerial photographs that appear on the ground surface.

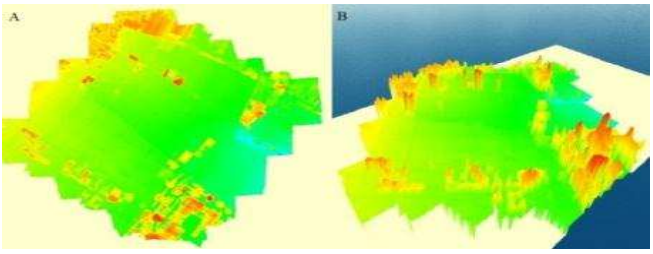

Fig. 6 Visualization of Digital Elevation Model by the use of Agisoft PhotoScan (A. 2D and B. 3D)

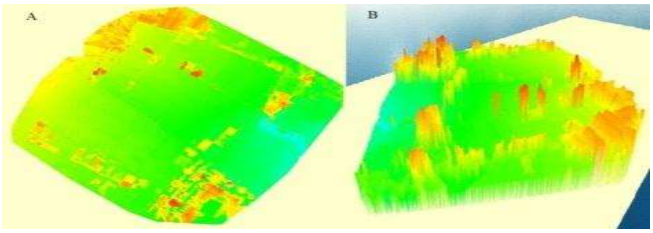

Fig. 7 Visualization of Digital Elevation Model by the use of Pix4D Mapper (A. 2D and B. 3D)

B. Test the Accuracy of Orthophoto Objects

DEM results horizontally with CE90 accuracy for AP. The accuracy obtained is 0.13854 m, with an RMSEr value of 0.09130 m (Table I) [17].

TABLE I
AGISOFT'S RMSER AND CE90 CALCULATION RESULTS

		RESIDUAL (m)		
Id	CODE	$(dx)^2$	$(dy)^2$	dx^2+dy^2
1	CP238	0.00170	0.02968	0.03138
2	CP237	0.00038	0.05214	0.05252
3	CP227	0.01133	0.05841	0.06974
4	CP236	0.01441	0.00301	0.01741
5	CP235	0.00058	0.00064	0.00122
6	CP234	0.00510	0.00510	0.01020
7	CP230	0.01314	0.00241	0.01555
8	CP231	0.01571	0.00695	0.02266
9	CP232	0.04775	0.00513	0.05288
10	CP233	0.00046	0.00039	0.00085
:	:	:	:	:
150	CP16	0.00000	0.00016	0.00016
			TOTAL	0.51677
			AVERAGE	0.00833
			RMSEr	0.09130
			CE90	0.13854

DEM results in vertical LE90 accuracy for APA obtained accuracy of 0.16930 m, with an RMSEz value of 0.27933 m (Table II) [17].

TABLE II
AGISOFT'S RMSEZ AND LE90 CALCULATION RESULTS

		RESIDUAL (m)		
Id	CODE	Z Field	Z Orthophoto	dz^2
1	CP181	480.36145	479.95100	0.16847
2	CP179	480.86102	480.60800	0.06402
3	CP178	481.54593	481.26800	0.07724
4	CP182	481.54779	481.33500	0.04528
5	CP183	481.86295	481.52900	0.11152
6	CP189	482.11505	482.03300	0.00673
7	CP187	482.37091	482.11200	0.06703
8	CP188	482.24170	482.03100	0.04439
9	CP186	482.14517	481.99700	0.02195
10	CP185	482.22965	482.04100	0.03559
:	:	:	:	:
150	CP279	497.28790	496.96200	0.10621
			TOTAL	0.77712
			AVERAGE	0.02866
			RMSEz	0.16930
			LE90	0.27933

DEM results in horizontal accuracy CE90 for PM Accuracy obtained 0.22384 m, with an RMSEr value of 0.14751 m (Table III) [10], [11], [17].

TABLE III
RMSER AND CE90 PIX4D MAPPER CALCULATION RESULTS

		RESIDUAL (m)		
Id	CODE	$(dx)^2$	$(dy)^2$	dx^2+dy^2
1	CP235	0.00126	0.00256	0.03138
2	CP234	0.00041	0.00860	0.00900
3	CP236	0.00237	0.00397	0.00634
4	CP230	0.13815	0.00001	0.13816
5	CP231	0.10932	0.00109	0.11041
6	CP232	0.03772	0.00788	0.04561
7	CP233	0.00072	0.00000	0.00073
8	CP227	0.07062	0.01569	0.08630
9	CP237	0.00204	0.03112	0.03316
10	CP238	0.00204	0.01876	0.02082
:	:	:	:	:
150	CP93	0.52196	0.06949	0.59145
			TOTAL	1.34901
			AVERAGE	0.02176
			RMSEr	0.14751
			CE90	0.22384

DEM results from vertical accuracy of LE90 for PM The accuracy obtained is 0.50924 m, with an RMSEz value of 0.30865 m, and the LE90 value does not exceed 0.75m (Table IV) [10], [11], [17].

TABLE IV
RMSEZ AND LE90 PIX4D MAPPER CALCULATION RESULTS

RESIDUAL (m)				
Id	CODE	Z Field	Z Orthophoto	dz^2
1	CP235	488.09686	488.02700	0.00488
2	CP234	487.86972	487.89000	0.00041
3	CP236	487.59116	487.55800	0.00110
4	CP230	486.74771	486.08400	0.44051
5	CP231	486.74100	486.03600	0.49702
6	CP232	486.89206	486.78600	0.01125
7	CP233	487.33521	487.38500	0.00248
8	CP227	488.38580	487.48700	0.80785
9	CP237	488.07739	487.89000	0.03512
10	CP238	488.36346	488.23600	0.01625
:	:	:	:	:
150	CP93	485.29550	483.58000	2.94295
			TOTAL	5.90648
			AVERAGE	0.09527
			RMSEz	0.30865
			LE90	0.50924

C. *Orthophoto Accuracy Test Results*

Conducted to determine the comparison of object distance values in the field and the orthophoto interpretation. The measurement results of the object are used as the basis for testing, and the measurement and interpretation data are calculated using the Commission Omission equation (Table V).

TABLE V
ORTHOPHOTO ACCURACY TEST RESULTS

id	Interpretation (m)		Field (m)	Difference (m)		Accuracy (%)		Description
	Agisoft	PIX4D		Agisoft	PIX4D	Agisoft	PIX4D	
1	9.77	9.78	9.78	-0.013	0.005	99.866	99.951	Fish Pond
2	14.22	14.31	14.34	-0.124	-0.032	99.137	99.774	Fish Pond
3	20.98	20.97	21.17	-0.194	-0.205	99.086	99.032	Fish Pond
4	17.98	17.99	18.49	-0.506	-0.502	97.265	97.286	Dormitory Length
7	36.65	36.64	35.97	0.678	0.668	98.115	98.143	Roof Length
9	8.79	8.78	8.70	0.090	0.080	98.965	99.076	Roof Width
10	9.96	10.02	9.97	-0.008	0.054	99.920	99.457	Roof Length
13	19.46	19.51	19.54	-0.084	-0.031	99.568	99.840	Office Length
14	1.77	1.74	1.70	0.068	0.043	96.007	97.484	Deker Length
15	1107	11.05	11.17	-0.103	-0.118	99.074	98.945	House Length
6	15.98	16.08	15.82	0.156	0.256	99.015	98.383	Dormitory Length
17	5.04	5.06	4.95	0.090	0.109	98.189	97.806	House Length
18	19.77	19.73	19.55	0.217	0.178	98.890	99.088	House Length
19	15.05	15.08	16.10	-1.047	-1.023	93.496	93.646	Dormitory Width
20	15.12	15.02	15.20	-0.078	-0.185	99.490	98.783	Dormitory Width
22	30.77	31.03	30.95	-0.183	0.080	99.407	99.743	Gutter Length
23	8.47	8.54	8.54	-0.067	-0.003	99.219	99.964	House Length
24	8.74	8.67	8.60	0.145	0.075	98.319	99.130	House Length
25	8.32	8.39	8.98	-0.661	-0.590	92.642	93.428	Road Width
26	6.11	6.19	6.17	-0.056	0.021	99.087	99.665	Road Width
27	4.02	4.03	4.08	-0.060	-0.052	98.528	98.722	Field Width
28	1.89	1.81	1.82	0.069	-0.009	96.224	99.529	Trench Wall Length
29	83.29	83.32	83.02	0.274	0.303	99.670	99.635	Fish Pond
30	14.01	14.02	13.94	0.068	0.078	99.510	99.440	Field Width
0	27.98	27.97	27.85	0.127	0.116	99.544	99.583	Field Length

Table V shows the difference between the measurement results and the interpretation of objects on orthophoto. The lowest was at AP at 0.008 m and PM at 0.003 m, the highest at AP at 1,047 m, and PM at 1,023 m. Calculating the accuracy percentage using the equation of the commission method obtained an average of AP and PM software > 90% with accuracy > 85%. This shows that the interpretation results are accepted overall because they meet the minimum requirements for the accuracy test and high accuracy values. The results of the comparison of the CE90 and LE90 horizontal and vertical geometries from the calculation of the AP and PM software Tabel VI.

TABLE VI
COMPARISON OF HORIZONTAL AND VERTICAL GEOMETRY ACCURACY

Horizontal accuracy (m)			Vertical accuracy (m)		
Caption	Agisoft	PIX4D	Caption	Agisoft	PIX4D
RMSEr	0.091	0.148	RMSEz	0.169	0.309
CE90	0.139	0.224	LE90	0.279	0.509

Based on Table 6, the AP software values RMSEr 0.091 m and CE90 0.139 m, while the PM software values RMSEr 0.148 m and CE90 0.224 m. The results of the CE90 value on a scale of 1:1000 class 1 with a maximum error of < 0.2 m (orthophoto horizontal position < 0.2 m). The AP software values RMSEz 0.169 m and LE90 0.279 m, while the PM software values RMSEz 0.309 m and LE90 0.509 m. Based on the value of LE90 scale 1:1000, class 2 maximum error < 0.30 m and class 3 maximum error < 0.5 m according to the RBI map already meets the standard of accuracy. The results of comparing the accuracy of the geometry of the AP software have a good accuracy value compared to the PM software.

IV. CONCLUSION

The results of processing aerial photos with AP and PM software in the form of Orthophoto are the same as the actual object shapes in the field and visually produce DEM in the form of 2D and 3D. The aerial photo accuracy test results using

AP software have RSEr values of 0.091 and CE90 0.139 m, while PM values of RSEr 0.148 and CE90 are 0.224 m. Based on the CE90 value on a scale of 1:1000 class 1 the maximum error is < 0.2 m. The AP software values RMSEz 0.169 and LE90 0.279 m, while the PM software values RMSEz 0.309 and LE90 0.509 m. The results of the LE90 value on a scale of 1:1000, class 2 maximum error < 0.30 m, and class 3 maximum error < 0.5 m according to the RBI map already meet the standard of accuracy. The calculation of the accuracy of the orthophoto and DEM data shows that the AP software has a better accuracy value than the PM software.

ACKNOWLEDGMENT

The Indonesian Domestic Lecturer Excellence Scholarship Education Fund Management Institute (LPDP-BUDI DN) of the Ministry of Finance of the Republic of Indonesia provided funding for this study.

REFERENCES

[1] H. A. Akpo *et al.*, "Trees , Forests and People Accuracy of tree stem circumference estimation using close range photogrammetry : Does point-based stem disk thickness matter ?," *Trees, For. People*, vol. 2, no. July, p. 100019, 2020, doi: 10.1016/j.tfp.2020.100019.

[2] V. Č. Aksamitauskas, "The surface modelling based on UAV Photogrammetry and qualitative estimation," *MEASUREMENT*, 2015, doi: 10.1016/j.measurement.2015.04.018.

[3] A. R. Bankert, E. H. Strasser, C. G. Burch, and M. D. Correll, "An open-source approach to characterizing Chihuahuan Desert vegetation communities using object-based image analysis," *J. Arid Environ.*, no. September, p. 104383, 2020, doi: 10.1016/j.jaridenv.2020.104383.

[4] J. Enciso *et al.*, "Validation of agronomic UAV and fi eld measurements for tomato varieties," *Comput. Electron. Agric.*, vol. 158, no. October 2018, pp. 278–283, 2019, doi: 10.1016/j.compag.2019.02.011.

[5] R. Freeland, B. Allred, N. Eash, L. Martinez, and D. Wishart, "Agricultural drainage tile surveying using an unmanned aircraft vehicle paired with Real-Time Kinematic positioning — A case study," *Comput. Electron. Agric.*, vol. 165, no. July, p. 104946, 2019, doi: 10.1016/j.compag.2019.104946.

[6] F. Giannetti, G. Chirici, T. Gobakken, E. Næsset, D. Travaglini, and S. Puliti, "Remote Sensing of Environment A new approach with DTM-independent metrics for forest growing stock prediction using UAV photogrammetric data," *Remote Sens. Environ.*, vol. 213, no. June 2017, pp. 195–205, 2018, doi: 10.1016/j.rse.2018.05.016.

[7] J. A. Gonçalves and R. Henriques, "ISPRS Journal of Photogrammetry and Remote Sensing UAV photogrammetry for topographic monitoring of coastal areas," vol. 104, pp. 101–111, 2015, doi: 10.1016/j.isprsjprs.2015.02.009.

[8] C. A. V. J, J. D. R. D, and C. A. R. R, "Jo ur l P re of," *J. Struct. Geol.*, p. 104214, 2020, doi: 10.1016/j.jsg.2020.104214.

[9] X. Jin, S. Liu, F. Baret, M. Hemerlé, and A. Comar, "Remote Sensing of Environment Estimates of plant density of wheat crops at emergence from very low altitude UAV imagery," *Remote Sens. Environ.*, vol. 198, pp. 105–114, 2017, doi: 10.1016/j.rse.2017.06.007.

[10] M. Moussa, A. Degré, C. Debouche, and J. Lisein, "Geomorphology The evaluation of unmanned aerial system-based photogrammetry and terrestrial laser scanning to generate DEMs of agricultural watersheds," *Geomorphology*, vol. 214, pp. 339–355, 2014, doi: 10.1016/j.geomorph.2014.02.016.

[11] J. Ramon, A. Reyes-menendez, and P. Palos-sanchez, "Mapping multispectral Digital Images using a Cloud Computing software : applications from UAV images," *Heliyon*, no. January, p. e01277, 2019, doi: 10.1016/j.heliyon.2019.e01277.

[12] M. Rusnák, J. Sládek, A. Kidová, and M. Lehotský, "Template for high-resolution river landscape mapping using UAV technology," *measurement*, 2017, doi: 10.1016/j.measurement.2017.10.023.

[13] S. Sankaran, L. R. Khot, R. Sinha, and J. J. Quiro, "High resolution aerial photogrammetry based 3D mapping of fruit crop canopies for precision inputs management," no. xxxx, pp. 1–13, 2021, doi: 10.1016/j.inpa.2021.01.006.

[14] A. Shirzadifar, M. Maharlooei, S. G. Bajwa, P. G. Oduor, and J. F. Nowatzki, "ScienceDirect Mapping crop stand count and planting uniformity using high resolution imagery in a maize crop," *Biosyst. Eng.*, vol. 200, pp. 377–390, 2020, doi: 10.1016/j.biosystemseng.2020.10.013.

[15] M. Syifa, P. R. Kadavi, S. J. Park, and C. Lee, "A Survey of Sediment Fineness and Moisture Content in the Soyang Lake Floodplain Using GPS Data," *Engineering*, vol. 7, no. 2, pp. 252–259, 2021, doi: 10.1016/j.eng.2020.12.011.

[16] S. N. Kuiry, "Assessing the accuracy of high-resolution topographic data generated using freely available packages based on SfM-MVS approach," *measurement*, 2018, doi: 10.1016/j.measurement.2018.04.043.

[17] J. X. Leon, C. M. Roelfsema, M. I. Saunders, and S. R. Phinn, "Geomorphology Measuring coral reef terrain roughness using ' Structure-from-Motion ' close-range photogrammetry," *Geomorphology*, vol. 242, pp. 21–28, 2015, doi: 10.1016/j.geomorph.2015.01.030.

[18] C. Bayliss, A. A. Juan, C. S. M. Currie, and J. Panadero, "Jou rna," *Appl. Soft Comput. J.*, p. 106280, 2020, doi: 10.1016/j.asoc.2020.106280.

[19] B. Bera, D. Chattaraj, and A. K. Das, "Jou rna," *Comput. Commun.*, 2020, doi: 10.1016/j.comcom.2020.02.011.

[20] A. Castellini, D. Bloisi, J. Blum, F. Masillo, and A. Farinelli, "Multivariate sensor signals collected by aquatic drones involved in water monitoring : A complete dataset," *Data Br.*, vol. 30, p. 105436, 2020, doi: 10.1016/j.dib.2020.105436.

[21] A. Jolfaei, "Jou rna lP pro of," *Comput. Commun.*, 2020, doi: 10.1016/j.comcom.2020.02.055.

[22] R. Kellermann, T. Biehle, and L. Fischer, "Transportation Research Interdisciplinary Perspectives Drones for parcel and passenger transportation : A literature review ☆," *Transp. Res. Interdiscip. Perspect.*, no. xxxx, p. 100088, 2019, doi: 10.1016/j.trip.2019.100088.

[23] S. H. Kim, "Journal of Air Transport Management Choice model based analysis of consumer preference for drone delivery service," *J. Air Transp. Manag.*, vol. 84, no. September 2019, p. 101785, 2020, doi: 10.1016/j.jairtraman.2020.101785.

[24] L. Di, P. Pugliese, F. Guerriero, and G. Macrina, "ScienceDirect Using drones for parcels delivery process Using parcels delivery process Using drones drones for for parcels delivery," *Procedia Manuf.*, vol. 42, pp. 488–497, 2019, doi: 10.1016/j.promfg.2020.02.043.

[25] P. L. Gonzalez-r, D. Canca, J. L. Andrade-pineda, M. Calle, and J. M. Leon-blanco, "Truck-drone team logistics : A heuristic approach to multi-drop route planning," *Transp. Res. Part C*, vol. 114, no. July 2019, pp. 657–680, 2020, doi: 10.1016/j.trc.2020.02.030.

[26] T. Kirschstein, "Comparison of energy demands of drone-based and ground-based parcel delivery services," *Transp. Res. Part D*, vol. 78, p. 102209, 2020, doi: 10.1016/j.trd.2019.102209.

[27] H. Lo *et al.*, "Field test of beach litter assessment by commercial aerial drone," *Mar. Pollut. Bull.*, vol. 151, no. November 2019, p. 110823, 2020, doi: 10.1016/j.marpolbul.2019.110823.

[28] X. Lu, X. Liu, Y. Li, Y. Zhang, and H. Zuo, "Simulations of airborne collisions between drones and an aircraft windshield," *Aerosp. Sci. Technol.*, vol. 1, p. 105713, 2020, doi: 10.1016/j.ast.2020.105713.

[29] M. Michels, C. Von Hobe, and O. Musshoff, "A trans-theoretical model for the adoption of drones by large-scale German farmers," *J. Rural Stud.*, no. October 2017, pp. 1–9, 2020, doi: 10.1016/j.jrurstud.2020.01.005.

[30] A. Mirzaeinia, M. Hassanalian, K. Lee, and M. Mirzaeinia, "Energy conservation of V-shaped swarming fixed-wing drones through position reconfiguration," *Aerosp. Sci. Technol.*, vol. 94, p. 105398, 2019, doi: 10.1016/j.ast.2019.105398.

[31] B. Mishra, D. Garg, P. Narang, and V. Mishra, "Jou rna lP pro of," *Comput. Commun.*, 2020, doi: 10.1016/j.comcom.2020.03.012.

[32] S. Poikonen, B. Golden, and B. Golden, "Multi-visit Drone Routing Problem," *Comput. Oper. Res.*, p. 104802, 2019, doi: 10.1016/j.cor.2019.104802.

[33] M. H. D. Saria and M. F. Al-sa, "Data in brief DroneRF dataset : A dataset of drones for RF- based detection , classi fi cation and identi fi cation," vol. 26, 2019, doi: 10.1016/j.dib.2019.104313.

[34] S. Sciancalepore *et al.*, "PiNcH : an Effective , Efficient , and Robust Solution to Drone Detection via Network Traffic Analysis," *Comput. Networks*, p. 107044, 2019, doi: 10.1016/j.comnet.2019.107044.

[35] M. Unal, E. Bostanci, and E. Sertalp, "Distant Augmented Reality : Bringing a new dimension to user experience using drones," *Digit.*

Appl. Archaeol. Cult. Herit., p. e00140, 2020, doi: 10.1016/j.daach.2020.e00140.

[36] J. Yaacoub and O. Salman, "Security Analysis of Drones Systems : Attacks , Limitations , and Recommendations," *Internet of Things*, p. 100218, 2020, doi: 10.1016/j.iot.2020.100218.

[37] A. Yudo, G. Jati, A. Octavian, and W. Jatmiko, "Switching target communication strategy for optimizing multiple pursuer drones performance in immobilizing Kamikaze multiple evader drones," *ICT Express*, no. xxxx, 2020, doi: 10.1016/j.icte.2020.03.007.

[38] X. Zhu, T. J. Pasch, and A. Bergstrom, "Technology in Society Understanding the structure of risk belief systems concerning drone delivery : A network analysis," *Technol. Soc.*, vol. 62, no. April, p. 101262, 2020, doi: 10.1016/j.techsoc.2020.101262.

[39] A. Triantafyllou *et al.*, "3-D digital outcrop model for analysis of brittle deformation and lithological mapping (Lorette cave , Belgium)," *J. Struct. Geol.*, vol. 120, no. July 2018, pp. 55–66, 2019, doi: 10.1016/j.jsg.2019.01.001.

[40] P. Zhu, G. Zhang, B. Zhang, and H. Wang, "Catena Variation in soil surface roughness under di ff erent land uses in a small watershed on the Loess Plateau , China," *Catena*, vol. 188, no. September 2019, p. 104465, 2020, doi: 10.1016/j.catena.2020.104465.